

1           Chemical Characterization of Secondary Organic  
2           Aerosol Constituents from Isoprene Ozonolysis in the  
3           Presence of Acidic Aerosol

4  
5     *Matthieu Riva<sup>a</sup>, Sri Hapsari Budisulistiorini<sup>a</sup>, Zhenfa Zhang<sup>a</sup>, Avram Gold<sup>a</sup> and Jason D.*  
6     *Surratt<sup>a\*</sup>*

7  
8     <sup>a</sup> Department of Environmental Sciences and Engineering, Gillings School of Global Public  
9     Health, The University of North Carolina at Chapel Hill, Chapel Hill, NC, United States

10  
11    \* Corresponding Author: Email - [surratt@unc.edu](mailto:surratt@unc.edu); Phone – 1-(919)-966-0470

12  
13    **HIGHLIGHTS**

- 14       - Acidified sulfate aerosol enhances production of SOA from isoprene ozonolysis.  
15       - Isoprene ozonolysis in the presence of acidic aerosol yields 2-methyltetrols.  
16       - Unique organosulfates (OSs) are characterized from isoprene ozonolysis.  
17       - 2-Methyltetrols and OSs may originate from heterogeneous reaction of peroxides.  
18       - Isoprene ozonolysis yields on average 14% of isoprene-derived OSs in field samples.

19    **KEYWORDS**

20    SOA, ozonolysis, isoprene, organosulfates, 2-methyltetrols

21

22 **ABSTRACT**

23 Isoprene is the most abundant non-methane hydrocarbon emitted into Earth's atmosphere and  
24 is predominantly derived from terrestrial vegetation. Prior studies have focused largely on the  
25 hydroxyl (OH) radical-initiated oxidation of isoprene and have demonstrated that highly  
26 oxidized compounds, such as isoprene-derived epoxides, enhance the formation of secondary  
27 organic aerosol (SOA) through heterogeneous (multiphase) reactions on acidified sulfate  
28 aerosol. However, studies on the impact of acidified sulfate aerosol on SOA formation from  
29 isoprene ozonolysis are lacking and the current work systematically examines this reaction.  
30 SOA was generated in an indoor smog chamber from isoprene ozonolysis under dark  
31 conditions in the presence of non-acidified or acidified sulfate seed aerosol. The effect of OH  
32 radicals on SOA chemical composition was investigated using diethyl ether as an OH radical  
33 scavenger. Aerosols were collected and chemically characterized by ultra performance liquid  
34 chromatography/electrospray ionization high-resolution quadrupole time-of-flight mass  
35 spectrometry (UPLC/ESI-HR-QTOFMS) and gas chromatography/electron impact ionization-  
36 mass spectrometry (GC/EI-MS). Analysis revealed the formation of highly oxidized  
37 compounds, including organosulfates (OSs) and 2-methylterols, which were significantly  
38 enhanced in the presence of acidified sulfate seed aerosol. OSs identified in the chamber  
39 experiments were also observed and quantified in summertime fine aerosol collected from  
40 two rural locations in the southeastern United States during the 2013 Southern Oxidant and  
41 Aerosol Study (SOAS).

42

43

## 44 1. INTRODUCTION

45 The largest mass fraction of fine particulate matter ( $\text{PM}_{2.5}$ , aerosol with aerodynamic  
46 diameters  $\leq 2.5 \mu\text{m}$ ) is generally organic, dominated by secondary organic aerosol (SOA)  
47 formed from the gas-phase oxidation of volatile organic compounds (VOCs). Although SOA  
48 contributes a large portion (20–90%) of the total  $\text{PM}_{2.5}$  mass, for the most part current models  
49 under-predict SOA mass (Kroll and Seinfeld, 2008; Hallquist et al., 2009). Biogenic VOCs  
50 (BVOCs), such as isoprene and monoterpenes, are typically the most abundant SOA  
51 precursors, especially in regions of dense terrestrial vegetation (Guenther et al., 2006).

52 Isoprene (2-methyl-1,3-butadiene,  $\text{C}_5\text{H}_8$ ) is the most abundant non-methane hydrocarbon  
53 emitted into the troposphere with emissions exceeding  $500 \text{ Tg yr}^{-1}$  (Guenther et al., 2006).  
54 The principal atmospheric degradation pathway of isoprene is oxidation by hydroxyl (OH)  
55 radical (Atkinson, 1997; Edney et al., 2005; Kroll et al., 2006), which along with oxidation by  
56 nitrate ( $\text{NO}_3$ ) radical and ozone ( $\text{O}_3$ ), accounts for up to 50% of the SOA budget (Henze and  
57 Seinfeld, 2006). Before 2004, SOA formation from atmospheric oxidation of isoprene was  
58 considered insignificant (Kamens et al., 1982; Pandis et al., 1991) because of the low  
59 molecular weight and high volatility of its known oxidation products and as a consequence,  
60 isoprene was not included in SOA models. However, the identification by Claeys and  
61 coworkers of 2-methyltetrols (Claeys et al., 2004a) and  $\text{C}_5$ -alkene triols (Wang et al., 2005) in  
62 ambient  $\text{PM}_{2.5}$  collected in the Amazon caused a re-examination of the potential for isoprene  
63 oxidation to yield SOA. Since the 2-methyltetrols and  $\text{C}_5$ -alkene triols contain the isoprene  
64 skeleton, isoprene was proposed as their source, although the mechanisms and environmental  
65 conditions leading to these products as well as the formation of isoprene SOA were not  
66 evident. Research over the last decade has established that relative humidity (RH) (Nguyen et  
67 al., 2011), levels of nitrogen oxides ( $\text{NO}_x$ ) (Kroll et al., 2006; Chan et al., 2010) and aerosol  
68 acidity (Surratt et al., 2007a, b) have pronounced effects on isoprene SOA formation. Recent

69 studies show that increased aerosol acidity is a key variable in enhancing SOA formation  
70 through the acid-catalyzed reactive uptake and multiphase chemistry of the OH radical-  
71 initiated oxidation products of isoprene, particularly the isomeric isoprene epoxydiols  
72 (IEPOX) (Paulot et al., 2009; Surratt et al., 2010; Lin et al., 2012; Gaston et al., 2014). Acid-  
73 catalyzed particle-phase reactions of IEPOX have been shown to yield the 2-methyltetrols and  
74 C<sub>5</sub>-alkene triols as well as IEPOX-derived dimers observed in the Amazonian PM<sub>2.5</sub> (Surratt  
75 et al., 2010; Lin et al., 2012). Epoxides generated by OH radical oxidation of isoprene have  
76 also been shown to explain the formation known organosulfates (OSs) and oligomers  
77 measured in ambient PM<sub>2.5</sub> samples (Surratt et al., 2007a, 2008; Lin et al., 2014). Although  
78 research over the last decade has focused principally on OH radical-initiated oxidation of  
79 isoprene, some work has also demonstrated significant SOA formation from the NO<sub>3</sub> radical-  
80 initiated oxidation of isoprene (Ng et al., 2008).

81 The contribution of isoprene ozonolysis to the SOA budget had been concluded to be  
82 negligible (Hasson et al., 2001; Kleindienst et al. 2007; Sato et al., 2013) on the basis of a  
83 large number of studies reporting only volatile and semivolatile products, such as methyl  
84 vinyl ketone (MVK), methacrolein (MACR) or low molecular weight acids. However, the  
85 potential importance of isoprene ozonolysis as a pathway for SOA formation is supported by  
86 recent studies documenting the formation of highly oxidized products, including oligomers, in  
87 both gas and particulate phases (Nguyen et al., 2010; Inomata et al., 2014). Initial formation  
88 of isoprene primary ozonides leads to stabilized Criegee intermediates (sCIs), which can react  
89 to form OH radicals, undergo further oxidation or condense to form higher molecular weight  
90 products. The total yield of sCIs, including CH<sub>2</sub>OO radical and higher molecular weight  
91 fragments, was determined to be 0.26 (Hasson et al., 2001), and the yield of OH radicals to be  
92 0.25 - 0.27 (Atkinson et al., 1992). Formation of highly oxidized compounds, such as  
93 oligomeric hydroperoxides identified in recent studies (Nguyen et al., 2010; Inomata et al.,

94 2014), was proposed by the reaction of sCIs with organic ozonolysis products (e.g. carboxylic  
95 acids) of isoprene. Multiphase reactions of the oxidized products could thus make significant  
96 contributions to the yield of SOA from isoprene ozonolysis. With the exception of reports by  
97 Jang et al. (2002) and Czoschke et al. (2003), effects of varying composition and acidity of  
98 sulfate aerosols and the presence of OH scavengers on SOA generated from isoprene  
99 ozonolysis have not been systematically investigated, nor have efforts have been reported to  
100 identify products unique to isoprene ozonolysis in ambient PM<sub>2.5</sub> samples collected from  
101 isoprene-rich areas.

102 In this study we investigate isoprene ozonolysis in the presence of sulfate seed aerosol  
103 of varying acidity and composition with a focus on the formation of OSs and highly oxidized  
104 compounds. Because of the high yield of OH radicals from isoprene ozonolysis, experiments  
105 were performed both in the presence and absence of an OH radical scavenger in order to  
106 identify SOA constituents derived directly from ozonolysis. Filters collected from indoor  
107 smog chamber experiments were analyzed by ultra performance liquid chromatography/  
108 electrospray ionization high-resolution quadrupole time-of-flight mass spectrometry  
109 (UPLC/ESI-HR-QTOFMS) and gas chromatography/electron impact mass spectrometry  
110 (GC/EI-MS). PM<sub>2.5</sub> samples collected from ground sites at Look Rock, TN, and Centerville,  
111 AL, during the 2013 Southern Oxidant and Aerosol Study (SOAS) were also analyzed to  
112 identify OSs present in both field and chamber studies and quantify their contribution to  
113 ambient PM<sub>2.5</sub>. Comparison of lab and field data supports the potential importance of isoprene  
114 ozonolysis in the isoprene-derived SOA budget.

115

## 116 **2. EXPERIMENTAL SECTION**

117 **2.1 Smog Chamber Experiments.** Ten experiments were performed in the indoor  
118 environmental smog chamber at the University of North Carolina. The experimental setup and

119 analysis techniques used in this work were described in detail previously (Lin et al., 2012;  
120 Zhang et al., 2012). Briefly, experiments were carried out under dark and dry conditions ( $3.3$   
121  $\pm 0.25\%$ , RH) at  $296 \pm 1$  K in a  $10\text{-m}^3$  Teflon chamber. Experimental conditions are  
122 summarized in Table 1. Prior to each experiment, the chamber was flushed continuously with  
123 clean air for  $\sim 24$  hours until the particle mass concentration was  $< 0.01 \mu\text{g m}^{-3}$  to ensure that  
124 there were no pre-existing aerosol particles prior to injection of isoprene. Aerosol size  
125 distributions were continuously measured using a differential mobility analyzer (DMA, BMI  
126 model 2002) coupled to a mixing condensation particle counter (MCPC, BMI model 1710) in  
127 order to monitor aerosol number, surface area, and volume concentration within the chamber.  
128 Chamber flushing also reduced  $\text{O}_3$  and VOC concentrations below the detection limit ( $< 1$   
129 ppb for ozone and isoprene). Temperature and RH in the chamber were continuously  
130 monitored using a dew point meter (Omega Engineering Inc.).

131 A known quantity of isoprene (Sigma-Aldrich, 99%) was introduced into the chamber  
132 by passing a heated nitrogen ( $\text{N}_2$ ) stream through a heated glass manifold. In some  
133 experiments, diethyl ether was injected by the same procedure to serve as an OH scavenger.  
134 Concentrations of isoprene and diethyl ether were measured every 10 minutes using an online  
135 gas chromatography/flame ionization detector (GC-FID, Model CP-3800, Varian), which was  
136 calibrated using multiple injections of isoprene and diethyl ether. Approximately 100 ppb of  
137 isoprene was injected for each experiment, while 3.5 ppm of diethyl ether was introduced in  
138 the experiments performed in the presence of OH scavenger. Approximately 1 hour after  
139 isoprene injection, 120–150 ppb of  $\text{O}_3$  was introduced into the chamber using an  $\text{O}_3$  generator  
140 (Model L21, Pacific ozone).  $\text{O}_3$  concentration was monitored over the course of experiments  
141 using an UV photometric analyzer (Model 49P, Thermo-Environmental).

142 Non-acidified or acidified ammonium or magnesium sulfate seed aerosols were  
143 introduced two hours after  $\text{O}_3$  injection. Non-acidified seed aerosol was generated from 0.06

144 M magnesium sulfate ( $\text{MgSO}_4$ ) or ammonium sulfate ( $(\text{NH}_4)_2\text{SO}_4$ ) (aq) solutions and  
145 acidified seed aerosol from 0.06 M  $\text{MgSO}_4$  (aq) or  $(\text{NH}_4)_2\text{SO}_4$  (aq) + 0.06 M  $\text{H}_2\text{SO}_4$  (aq)  
146 solutions. Once aerosol volume concentrations stabilized ( $\sim 1$  hour after reaction), aerosols  
147 were collected onto 47-mm diameter Teflon filters (1.0- $\mu\text{m}$  pore size, Tisch Environmental,  
148 EPA  $\text{PM}_{2.5}$  membrane) for two hours at a sampling flow rate of  $25 \text{ L min}^{-1}$  to characterize  
149 particle-phase reaction products.

150 **2.2 Ambient  $\text{PM}_{2.5}$  Collection.**  $\text{PM}_{2.5}$  samples were collected during the 2013 SOAS  
151 campaign from 1 June to 15 July 2013 at Centerville, AL (CTR), and from 1 June to 17 July  
152 2013 at Look Rock, TN (LRK). Both sites are strongly influenced by isoprene emissions  
153 (Guenther et al., 2006), and isoprene oxidation appears to be one of the main SOA  
154 contributors (Budisulistiorini et al., 2015; Xu et al., 2015). At each site,  $\text{PM}_{2.5}$  samples were  
155 collected onto pre-baked  $8 \times 10$  in Tissuquartz™ Filters (Pall Life Sciences) with high-  
156 volume  $\text{PM}_{2.5}$  air samplers (Tisch Environmental) operated at  $1 \text{ m}^3 \text{ min}^{-1}$  using two sampling  
157 protocols described in detail elsewhere (Budisulistiorini et al. 2015). A total of 118 filters  
158 from CTR and 123 filters from LRK were analyzed to evaluate the contributions of OSs  
159 identified from isoprene ozonolysis on the isoprene-derived SOA budget.

160 **2.3 Aerosol-Phase Chemical Characterization.** Chemical characterization of SOA  
161 from isoprene ozonolysis was performed by UPLC/ESI-HR-Q-TOFMS (6520 Series, Agilent)  
162 operated in the negative ion mode and by GC/EI-MS (Hewlett-Packard, 5890 Series II).  
163 Operating conditions have been described in detail in elsewhere (Lin et al., 2012). Filters  
164 collected from smog chamber experiments were extracted with 22 mL of high-purity  
165 methanol (LC-MS CHROMASOLV-grade, Sigma-Aldrich) by sonication for 45 min. The  
166 methanol extracts were blown dry under a gentle  $\text{N}_2$  (g) stream at ambient temperature. Dried  
167 extracts were reconstituted in 2 mL methanol, divided into two equal portions and then blown  
168 dry.

169 For UPLC/ESI-HR-QTOFMS analysis, one of the dried extracts was reconstituted  
170 with 150  $\mu\text{L}$  of a 50:50 (v/v) solvent mixture of methanol (LC-MS CHROMASOLV-grade,  
171 Sigma-Aldrich) and high-purity water (Milli-Q, 18.2 M $\Omega$ ). 5  $\mu\text{L}$  aliquots were injected onto  
172 the UPLC column (Waters ACQUITY UPLC HSS T3 column, 2.1  $\times$  100 mm, 1.8  $\mu\text{m}$  particle  
173 size) and eluted at a flow rate of 0.3 mL min<sup>-1</sup> with a solvent mixture of methanol containing  
174 0.1% acetic acid (LC-MS CHROMASOLV-grade, Sigma-Aldrich) and water containing 0.1  
175 % acetic acid (LC-MS CHROMASOLV-grade, Sigma-Aldrich). OSs were characterized by  
176 high-resolution mass spectra to determine the composition of SOA constituents and structural  
177 information was obtained through acquisition of high-resolution tandem mass spectra (MS<sup>2</sup>)  
178 at a collision energy of 15 V. A mixture of 2-methyltetrol sulfate esters (C<sub>5</sub>H<sub>11</sub>O<sub>7</sub>S<sup>-</sup>)  
179 (Budisulistiorini et al., 2015) and 2-oxopropyl sulfate (hydroxyacetone sulfate ester;  
180 C<sub>3</sub>H<sub>5</sub>O<sub>5</sub>S<sup>-</sup>; SI Figures S1, S2) were synthesized in-house as authentic standards. Propyl  
181 sulfate (C<sub>3</sub>H<sub>7</sub>O<sub>4</sub>S<sup>-</sup>; electronic grade, City Chemical LLC) and 3-pinanol-2-hydrogen sulfate  
182 (C<sub>9</sub>H<sub>13</sub>O<sub>6</sub>S<sup>-</sup>; synthesized standard from Marianne Glasius's group) served as surrogate  
183 standards to quantify the remaining OSs.

184 The second portion of dried filter extract was trimethylsilylated by addition of 100  $\mu\text{L}$   
185 BSTFA + trimethylchlorosilane (99:1 (v/v), Supleco) and 50  $\mu\text{L}$  pyridine (Sigma-Aldrich,  
186 98%, anhydrous). The mixture was heated for 1 h at 70 °C and analyzed within 24 hours  
187 following trimethylsilylation. Analyses were performed by GC/EI-MS at 70 eV (Hewlett  
188 5890 Packard Series II Gas Chromatograph interfaced to a HP 5971A Series Mass Selective  
189 Detector, Econo-Cap<sup>TM</sup>-ECTM-5 column, 30 m  $\times$  0.25 mm  $\times$  0.25  $\mu\text{m}$ ). 2-Methyltetrols  
190 were quantified using the authentic standard (Budisulistiorini et al., 2015).

191 Filters collected from field studies were extracted using the protocol described above;  
192 however, prior to drying, extracts were filtered through 0.2- $\mu\text{m}$  PTFE syringe filters (Pall Life  
193 Science, Acrodisc) to remove insoluble particles or quartz filter fibers.



194 **3. RESULTS AND DISCUSSION**

195 **3.1 OS formation.** In addition to four sulfate esters previously reported from  
196 photooxidation of isoprene under low- or high-NO<sub>x</sub> conditions (Surratt et al., 2008) (Table 1),  
197 12 products unique to ozonolysis were identified and quantified (Table 2).

198 Negative ion UPLC/ESI-HR-QTOFMS analysis of filter extracts provides excellent  
199 sensitivity for the detection of OSs, which yield intense [M-H]<sup>-</sup> ions (Surratt et al., 2008;  
200 Hansen et al., 2014) and show characteristic product ions at *m/z* 80 (SO<sub>3</sub><sup>\*-</sup>), 81 (HSO<sub>3</sub><sup>-</sup>) or 97  
201 (HSO<sub>4</sub><sup>-</sup>) in MS<sup>2</sup> spectra. Accurate mass measurements of parent and major product ions,  
202 number of isomers/isobars for each parent mass, MS<sup>2</sup> spectra and proposed structures are  
203 given in Figure 1 and Supporting Information (SI; Figures S3 and S4 and Table S1). 2-  
204 Methyltetrol sulfate esters (isomers not specified) and 2-oxopropyl sulfate were identified by  
205 comparison with the authentic standards; other structures have been tentatively assigned  
206 based on accurate mass measurements of parent and product ions and comparison of MS<sup>2</sup>  
207 fragmentation patterns with those of structurally similar OSs available in the literature such as  
208 the OSs at *m/z* 169, 213, and 215 (Surratt et al., 2007a; Gomez-Gonzalez et al., 2008), the OS  
209 at *m/z* 199 (Zhang et al., 2012), and the OS at *m/z* 183 (Safi Shalamzari et al., 2013). Figures  
210 1a–f illustrate the assignment of structures for the major OSs identified in both laboratory-  
211 generated and ambient SOA.

212 Two isobaric parent ions with the composition C<sub>4</sub>H<sub>7</sub>O<sub>6</sub>S<sup>-</sup> (*m/z* 183) in Figure 1a and b  
213 lose bisulfate (*m/z* 97) as the base peak fragment ion and can thus be identified as OSs with a  
214 labile proton β to the sulfate group; proposed fragmentation schemes for these two isomers  
215 can be found in Figures S3a and S3b. An OS with this composition has been reported in  
216 ambient PM<sub>2.5</sub> (Safi Shalamzari et al., 2013), and was assigned as the O<sup>3</sup>-sulfate ester of 3,4-  
217 dihydroxybutan-2-one based by comparison of its MS<sup>2</sup> spectrum with the MS<sup>2</sup> spectrum of a  
218 synthetic mixture of the O<sup>3</sup>- + O<sup>4</sup>-sulfate esters of 3,4-dihydroxybutan-2-one. While these

219 data were acquired on an Orbitrap mass spectrometer and a QTOFMS was employed in this  
220 study, the key product ions at  $m/z$  165 [ $M - H_2O$ ], 153 [ $M - CH_2O$ ] and 97 [ $HSO_4^-$ ] are  
221 common to both analyses and in accord with monosulfated 3,4-diol isomers of of 3,4-  
222 dihydroxybutan-2-one. In Figure 1b, an additional product ion appears in the  $MS^2$  spectrum of  
223 the late-eluting peak at  $m/z$  85 [ $M - H_2SO_4$ ]. Loss of  $H_2SO_4$  as a neutral fragment to give 3-  
224 oxobut-1-en-1-olate, a homolog of the known, stable enolate of malondialdehyde, would be  
225 favored by the  $O^3$ -sulfate ester (Figure S3b). In addition, the loss of formaldehyde to give the  
226 product ion at  $m/z$  153 is also favored. The favorability of both fragmentation pathways by the  
227  $O^3$ -ester might be expected to result in reduced parent ion intensity relative to the  $O^4$ -ester at a  
228 given collisional energy, as is observed in the  $MS^2$  spectrum (Figure 1b). On this basis  $O^3$ -  
229 and  $O^4$ -sulfate ester structural assignments have been made for the late- and early-eluting  
230 products, respectively.

231 Regarding a possible source of the  $m/z$  183 isomers, the epoxide of MVK (1-oxiran-2-yl-  
232 ethan-1-one) has been proposed as the precursor (Safi Shalamzari et al. 2013). The oxirane is  
233 unlikely to be a product of gas-phase ozonolysis of MVK (Neeb et al., 1998). However,  
234 uptake onto sulfate aerosols of gas-phase organic peroxides from the reaction of sCIs with  
235 carboxylic acids (Nguyen et al., 2010; Inomata et al., 2014) is a potential source of aerosol  
236 phase oxidants either by oxidation of sulfate to  $SO_4^{-\bullet}$  or via generation of  $H_2O_2$  (Chen et al.,  
237 2008). An  $m/z$  183 product has been identified from sulfate radical oxidation of MVK in bulk  
238 aqueous solution (Schindelka et al., 2013), suggesting aerosol-phase oxidation by  $SO_4^{-\bullet}$  is  
239 possible. Hence, aerosol-phase oxidation by  $SO_4^{-\bullet}$  or acid-catalyzed ring opening of  
240 peroxide-generated oxiranes (Iinuma et al., 2009; Surratt et al., 2010) are plausible routes to  
241  $m/z$  183 and other OSs. Sulfate addition to alkenes or aldehyde groups under strong acid  
242 conditions (Liggio et al., 2006; Surratt et al., 2007a) could also be considered as an alternative  
243 pathway to some products.

244 Two ions were identified at  $m/z$  197 ( $C_5H_9O_6S^-$ ). OSs with this nominal mass have been  
245 tentatively identified as sulfate esters of  $C_5$ -alkene triols from uptake of isoprene oxidation  
246 products onto acidified sulfate aerosol (Surratt et al., 2007a). However, molecular  
247 compositions were not verified by accurate mass measurements and  $MS^2$  spectra were not  
248 reported.  $MS^2$  spectra of products at  $m/z$  197 observed in our ozonolysis experiment (Figures  
249 1c, d; Figures S3c, d) are consistent with a tentative assignment as isomeric sulfate esters of  
250 the alkene triol 1,4-dihydroxy-3-methylbutan-2-one. The early eluting sulfate is assigned the  
251 structure 4-hydroxy-2-methyl-3-oxobutyl sulfate based on the loss of the neutral fragment  
252  $C_2H_4O_2$  (2-hydroxyacetaldehyde) to give a product ion at  $m/z$  137 ( $C_3H_5O_4S^-$ ) (Figure S3c),  
253 and the late-eluting isomer is assigned as the 2-oxo sulfate based on the loss of 60 mass units  
254 ( $C_3H_8O$ ) to give a product ion at  $m/z$  139 ( $C_2H_3O_5S^-$ ) (Figure S3d). Prominent ions are  
255 present for bisulfate ( $m/z$  97),  $SO_3^{-\bullet}$  ( $m/z$  80) and loss of formaldehyde ( $m/z$  167) in  $MS^2$   
256 spectra of both early- and late-eluting isomers, consistent with the proposed OS structures.

257 An ion at  $m/z$  199 with composition  $C_5H_{11}O_7S^-$  (Figure 1e) has been observed as a  
258 component of SOA generated by the reactive uptake of oxidation products of 2-methyl-3-  
259 buten-2-ol (MBO) on both acidified and neutral ammonium sulfate aerosols (Zhang et al.,  
260 2012) and tentatively identified as 2,3-dihydroxy-3-methylbutyl sulfate. Bisulfate is the only  
261 significant product ion in the  $MS^2$ , which is identical to the  $MS^2$  spectrum obtained from the  
262 ozonolysis experiment in this study (Figure 1e). Since terminal hydroxymethylene groups in  
263 possible isobaric structures would be expected to result in  $MS^2$  pathways yielding more  
264 complex fragmentation patterns, the structural assignment 2,3-dihydroxy-3-methylbutyl  
265 sulfate is tentatively made for this ozonolysis product. The parent ion at  $m/z$  215 ( $C_5H_{11}O_7S^-$ )  
266 has been identified as a 2-methyltetrol sulfate isomer (or isomer mixture) by comparison of  
267 the retention time and  $MS^2$  spectrum with the authentic standard mixture. Its  $MS^2$  spectrum is  
268 characterized by loss of bisulfate as the only significant fragmentation (Figures 1f, S3f).

269 All the parent ions of products in Tables 1 and 2 show an intense product ion at  $m/z$  97,  
270 characteristic of sulfate esters with a labile proton in proximity to the sulfate group. Two ions  
271 are present at  $m/z$  153 with composition  $C_3H_5O_5S^-$ .  $MS^2$  spectra of earlier- and later-eluting  
272 products are presented in Figures S4a and S4b, respectively. Products with this composition,  
273 tentatively identified as the sulfate ester of hydroxyacetone (2-oxopropyl sulfate), a known  
274 oxidation product of isoprene, have been observed in SOA from uptake of isoprene oxidation  
275 products onto acidic sulfate seed aerosol (Surratt et al., 2007a) and from bisulfate radical  
276 oxidation of isoprene in bulk solution (Schindelka et al., 2013). The later-eluting product was  
277 identified as 2-oxopropyl sulfate by matching retention time and  $MS^2$  with an authentic  
278 sample. The  $MS^2$  of the earlier-eluting product was identical (Figures S4a1, 4a2), yielding  
279 product ions for loss of bisulfate, bisulfite and  $SO_3$  and therefore not informative regarding  
280 structural identification. The tautomer of 2-oxopropyl sulfate, 1-oxopropan-2-yl sulfate, is a  
281 possible isobaric structure.

282 Only one of two ions at  $m/z$  169 ( $C_3H_5O_6S^-$ ) was present in sufficient abundance for  
283 acquisition of an  $MS^2$  spectrum. The  $MS^2$  is not consistent with the  $MS^2$  reported for an  
284 authentic sample of the known lactic acid sulfate (Olson et al., 2011; Safi Shalamzari et al.,  
285 2013). Although the published spectrum was acquired on an instrument equipped with an ion  
286 trap source and complete correspondence to QTOFMS in this study might not be assumed, the  
287 product ions in the  $MS^2$  spectra in this study (Figure S4b) are incompatible with the lactic  
288 acid derivative. A potential candidate for  $m/z$  169 isomers observed here are the sulfate esters  
289 of glyceraldehyde (2,3-dihydroxypropanal), which is a known product from isoprene  
290 oxidation (Fang et al. 2012) and has been previously identified in  $PM_{2.5}$  samples collected  
291 from isoprene rich-regions (Surratt et al. 2008). The fragmentation pattern in Figure S4b is  
292 consistent with a mixture of isomeric glyceraldehyde sulfate esters. The product ion at  $m/z$   
293 137 ( $C_2HO_5S^-$ ), can be rationalized as the sulfate ester of hydroxy ketene. In the absence of

294 MS<sup>2</sup> data for both parent ions, however, an alternative explanation for one of the parent ions  
295 would be the sulfate ester of dihydroxyacetone (Paulot et al., 2009), which could also give the  
296 observed MS<sup>2</sup> (Figure S4b).

297 Parent ions at *m/z* 179 (C<sub>5</sub>H<sub>7</sub>O<sub>5</sub>S<sup>-</sup>) and 181 (C<sub>5</sub>H<sub>9</sub>O<sub>5</sub>S<sup>-</sup>) from isoprene oxidation have not  
298 been previously reported. The composition of the parent ion at *m/z* 179 indicates retention of  
299 the isoprene carbon skeleton. The MS<sup>2</sup> spectrum (Figure S4c) is characterized by product ions  
300 HSO<sub>4</sub><sup>-</sup>, HSO<sub>3</sub><sup>-</sup> and C<sub>4</sub>H<sub>7</sub>O<sub>4</sub>S<sup>-</sup> [(M - CO)]. The bisulfite product ion is characteristic of a  
301 labile proton α to the sulfate substituent, while bisulfate product ion indicates a labile proton  
302 accessible 2 or more carbons removed and the loss of CO indicates a terminal carbonyl group.  
303 The isomeric structures 4-oxo-3-(or 2-)-methyl-but-2-ene sulfate, sulfate esters of the reported  
304 isoprene oxidation products 4-hydroxy-2-(or 3-)-methylbut-2-enal (Baker et al., 2005), are  
305 compatible with the MS<sup>2</sup> data and hence are proposed as possible structures of the ion at *m/z*  
306 179. The bisulfate product ion and the loss of formaldehyde in MS<sup>2</sup> spectrum of the parent ion  
307 at *m/z* 181 (Figure S4d) suggest that a labile proton 2 or more carbons removed from the  
308 sulfate substituent and a terminal hydroxymethyl group are structural features. Sulfate esters  
309 of the known 1,4-, 1,2-, and 3,4-dihydroxy oxidation products of isoprene might yield the  
310 observed MS<sup>2</sup> trace. However, bisulfite is not present in the MS<sup>2</sup> spectrum, thus the *O*<sup>2</sup>-sulfate  
311 ester of 1,2-dihydroxy-2-methylbutene best explains the data (Figure S4d) and is suggested as  
312 the structure of the parent ion.

313 Parent ions at *m/z* 213 having the composition C<sub>5</sub>H<sub>9</sub>O<sub>7</sub>S<sup>-</sup> have been detected in ambient  
314 SOA collected at K-puszta, Hungary (Gómez-González et al., 2008) and in chamber studies  
315 of isoprene photooxidation (Surratt et al., 2008). Based on analysis of MS<sup>2</sup> and MS<sup>3</sup> data, the  
316 compounds observed at K-puszta were assigned as sulfate esters of 4,5-dihydroxypentanoic  
317 acid from fatty acid oxidation and 2,3-dihydroxypentanoic acid, a photoproduct of plant leaf  
318 volatiles (Gómez-González et al., 2008). The isoprene-derived OSs at *m/z* 213 were not

319 assigned structures and no full-scan or MS<sup>2</sup> mass spectra were given (Surratt et al., 2008). The  
320 MS<sup>2</sup> spectrum acquired in this study (Figure S4e) is characterized by product ions at *m/z* 183  
321 (M – CH<sub>2</sub>O), 139 (M – C<sub>3</sub>H<sub>6</sub>O<sub>2</sub>), and 97 (bisulfate), which are not compatible with either of  
322 the pentanoic acid derivatives reported by Gómez-González et al. (2008). A product retaining  
323 the isoprene carbon skeleton, 3,4-dihydroxy-3-methyl-2-oxobutylsulfate, could be anticipated  
324 to lose formaldehyde and hydroxyacetone as neutral fragments (Figure S4e) and this structure  
325 is tentatively assigned to the isoprene-derived OS.

326         Seven parent ions with 6 or more carbons not previously reported from isoprene  
327 ozonolysis were observed (Table 2). The products were mainly observed in experiments using  
328 acidified MgSO<sub>4</sub> seed aerosol (Table 2) and the low intensity of the parent ions precluded  
329 acquisition of MS<sup>2</sup> data. Formation of oligomers and their OS derivatives in the presence of  
330 MgSO<sub>4</sub> seed aerosol has been previously reported and potential involvements of Mg<sup>2+</sup> have  
331 been discussed (Lin et al., 2014); specifically, MgSO<sub>4</sub> aerosols do not effloresce at low-RH  
332 conditions and instead form gel-like chain structures of contact ion pairs (Chan et al., 2000).  
333 We tentatively propose that this phase state (gel-like chain structures) of MgSO<sub>4</sub> allows  
334 transient moieties to be held in close proximity to each other by coordination to Mg<sup>2+</sup> ions in  
335 the gel-like aerosol structure. Future work is needed to more fully resolve the effect of MgSO<sub>4</sub>  
336 seed aerosol. Consistent with previous work (Surratt et al., 2007b), acidity enhanced the  
337 formation of all OSs (Figure 2).

338         The products in Table 1 at *m/z* 153 (C<sub>3</sub>H<sub>5</sub>O<sub>5</sub>S<sup>-</sup>), 169 (C<sub>3</sub>H<sub>5</sub>O<sub>6</sub>S<sup>-</sup>), 213 (C<sub>5</sub>H<sub>9</sub>O<sub>7</sub>S<sup>-</sup>) and  
339 215 (C<sub>5</sub>H<sub>11</sub>O<sub>7</sub>S<sup>-</sup>), which have been observed during OH radical-initiated oxidation of isoprene  
340 (Surratt et al., 2007a) are also observed in the ozonolysis experiments in the presence of OH  
341 radical scavenger, although the radical scavenger reduces formation of all OSs. The high  
342 concentration of diethyl ether used in this study precludes residual OH radical as an  
343 explanation for these products at observed concentrations. Lack of authentic standards

344 prevents definitive conclusion as to whether the products at  $m/z$  153, 169 and 213 from  
345 photochemical oxidation and ozonolysis of isoprene are identical or are isobars. However, the  
346 sulfate ester at  $m/z$  215, which was generated in high yield in this study, has been confirmed  
347 as a sulfate ester of an isoprene-derived 2-methyltetrol diastereomer (2-methylerythritol or 2-  
348 methylthreitol) by comparison with an authentic standard mixture, indicating that both  
349 hydroxyl radical and ozonolysis may contribute to 2-methyltetrol sulfate derivatives in  
350 ambient fine aerosol.

351 **3.2 Formation of 2-Methyltetrols.** 2-Methylterols have been identified in SOA from  
352 reactive uptake of isoprene epoxydiol (IEPOX) isomers on sulfate seed aerosols (Surratt et al.,  
353 2010; Lin et al., 2012). One study has also reported the formation of the 2-methyltetrols from  
354 isoprene ozonolysis in the presence of non-acidified sulfate aerosol (Kleindienst et al., 2007).  
355 In the current ozonolysis study, large quantities of 2-methyltetrols were identified in SOA.  
356 Consistent with previous studies (Surratt et al., 2007b), the yield of 2-methyltetrols is highly  
357 dependent on the acidity and composition of the sulfate seed aerosol (Figure 3), with acidified  
358  $MgSO_4$  giving the highest yield. Kleindienst et al. (2007) attributed the formation of tetrols  
359 during ozonolysis to reaction of isoprene with OH radicals generated during the reaction,  
360 estimating that 16% of the OH radicals formed reacted with isoprene. Initial concentration of  
361 diethyl ether (35-fold higher than isoprene) prevents any reaction of OH radicals with  
362 isoprene. Indeed, OH radical oxidation of diethyl ether is 46-fold higher than that with  
363 isoprene in experimental conditions used in this work (Mellouki et al., 1995; Atkinson et al.,  
364 2006). The absence of  $C_5$ -alkene triols, 2-methylglyceric acid and 3-methyltetrahydrofuran-  
365 3,4-diols, established SOA markers of isoprene photooxidation (Surratt et al., 2010; Lin et  
366 al., 2012), also argues against the formation of 2-methyltetrols by OH radical oxidation.  
367 These observations along with the high ratio of 2-methyltetrols to IEPOX-derived OSs (Table  
368 1 and Figure 3), leads to the conclusion that isoprene ozonolysis in the presence of acidified

369 sulfate seed aerosol is a hitherto unrecognized source of 2-methyltetrols. Acid-catalyzed  
370 heterogeneous reactions with organic peroxides (Inomata et al., 2014) or H<sub>2</sub>O<sub>2</sub> (Chen et al.,  
371 2008), likely to be present in acidic SOA as discussed above, is a possible route for formation  
372 of the 2-methyltetrols. Aerosol-phase acid-catalyzed oxidation of isoprene to the 2-  
373 methyltetrols has been proposed and demonstrated in the aqueous phase (Claeys et al.,  
374 2004b).

375 **3.3 Field measurements.** 13 of the 16 OSs identified in the chamber ozonolysis  
376 experiments (Tables 1 and 2) were detected in the ambient PM<sub>2.5</sub> samples from CTR and LRK  
377 sites during the 2013 SOAS campaign. As discussed above in the chemical characterization of  
378 parent ions, a number of organosulfates that have not been reported as photochemical  
379 oxidation products of isoprene are esters of known photochemical products. The significance  
380 of this observation with regard to whether these organosulfates are exclusively generated by  
381 ozonolysis via as yet unknown pathways or result from esterification of hydroxy substituents  
382 in the aerosol phase remains to be determined. Time profiles of OSs for CTR are shown in  
383 Figure 4 and for LRK, in Figure S5. The time profiles exclude the product at *m/z* 249, to  
384 which terpene photolysis may contribute substantially, and the OSs reported Table 1 such as  
385 2-methyltetrol sulfates (*m/z* 215), to which photochemically generated IEPOX may contribute  
386 substantially, but include the OSs in Table 2, which have not been reported in photochemical  
387 experiments. The average concentrations of the ambient OSs, excluding OSs as stipulated  
388 above, were  $18.3 \pm 12.3 \text{ ng m}^{-3}$  at CTR and  $21.3 \pm 20.7 \text{ ng m}^{-3}$  at LRK. Time profiles of the  
389 sum of all isoprene-derived OSs identified at LRK and CTR are presented in Figures 5 and  
390 S6, respectively. The sum of concentrations of OSs we attribute to isoprene ozonolysis during  
391 the 2013 SOAS is highly correlated with the sum of all isoprene-derived OSs ( $r^2 = 0.75$  for  
392 CTR and  $r^2 = 0.92$  for LRK). On average, OSs derived from isoprene ozonolysis represent  
393 14% of the sum of all isoprene-derived OSs quantified at both CTR and LRK. This is likely



394 an underestimate due to complete exclusion of  $m/z$  249 and OSs reported Table 1, which  
395 could be formed by other chemical processes, such as photooxidation of isoprene.

396 Correlation of on-line gas-phase  $O_3$  concentration with OSs is weak and suggests that  
397 formation of OSs occurred upwind of the sampling site, as demonstrated for other SOA  
398 tracers (Budisulistiorini et al., 2015). Since this study supports isoprene ozonolysis as an  
399 important source of 2-methylterols, correlation of 2-methyltetrols and OSs from isoprene  
400 ozonolysis was calculated and is presented in Figure 5 for both sampling sites. At LRK, a  
401 moderate correlation ( $r^2 = 0.40$ ) suggests a contribution to 2-methyltetrols from isoprene  
402 ozonolysis at this site during the 2013 SOAS campaign. Conversely, the weak correlation at  
403 CTR ( $r^2 = 0.18$ ) indicates a smaller role of isoprene ozonolysis in the formation of 2-  
404 methyltetrols at this site.

405

#### 406 4. CONCLUSIONS

407 In the present study, the impact of acidified sulfate aerosol on SOA composition  
408 arising from isoprene ozonolysis was systematically examined in smog chamber studies.  
409 Chemical characterization of SOA demonstrated substantial yields of OSs and 2-methylterols  
410 from ozonolysis of isoprene in the presence of acidified sulfate seed aerosol. The presence of  
411 an OH radical scavenger in chamber studies resulted in decreased concentrations of products  
412 that could be identified, indicating a contribution to oxidation by OH radicals. Nevertheless,  
413 substantial particle-phase concentrations of both OSs and 2-methyltetrols from ozonolysis in  
414 the presence of an OH scavenger suggest that the SOA yields from isoprene ozonolysis may  
415 be underestimated by current models. Furthermore, SOA yields from isoprene ozonolysis  
416 have hitherto been determined either without seed particles (Sato et al., 2013) or in the  
417 presence of non-acidified aerosols (Kleindienst et al., 2007). Further supporting the  
418 conclusion that the contribution of ozonolysis to the isoprene-derived SOA budget is likely

419 underestimated, OSs identified in our chamber experiments but not previously reported as  
420 products of reactive uptake of photochemical isoprene oxidation were quantified in PM<sub>2.5</sub>  
421 samples collected from two rural sites in the southeastern U.S. SOA yields from isoprene  
422 ozonolysis have been reported to increase in the presence of acidified sulfate seed aerosol  
423 (Jang et al., 2002); however, SOA composition was not characterized and no hypotheses were  
424 offered with regard to mechanisms underlying this effect. A substantial yield of 2-  
425 methyltetrols in the presence of a large excess of OH scavenger supports isoprene oxidation  
426 by an alternative pathway, such as acid-catalyzed oxidation by organic peroxides in accord  
427 with a previous hypothesis (Claeys, 2004b). A potential source of organic peroxides in the  
428 aerosol phase is sCI oligomerization and subsequent uptake, recently reported by Inomata et  
429 al. (2014). Further investigation is required to understand how acidified sulfate seed aerosols  
430 take up organic peroxides from the gas phase and how particle-phase reactions might degrade  
431 organic peroxides into low-volatility products (e.g., OSs) in order to develop mechanisms of  
432 SOA formation from isoprene ozonolysis in the presence of acidified sulfate aerosol.

433

#### 434 **AUTHOR INFORMATION**

435 Corresponding author: Jason D. Surratt

436 Email: [surratt@unc.edu](mailto:surratt@unc.edu)

437 Phone: 1-(919)-966-0470

438

#### 439 **ACKNOWLEDGMENTS**

440 The authors wish to thank the Camille and Henry Dreyfus Postdoctoral Fellowship Program  
441 in Environmental Chemistry for their financial support. This work is also funded in part by  
442 the U.S. Environmental Protection Agency (EPA) grant R835404 and the National Science  
443 Foundation grant CHE-1404644. The contents of this publication are solely the responsibility

444 of the authors and do not necessarily represent the official views of the U.S. EPA. Further, the  
445 U.S. EPA does not endorse the purchase of any commercial products or services mentioned in  
446 the publication. The authors wish to thank Kasper Kristensen and Marianne Glasius  
447 (Department of Chemistry, Aarhus University, Denmark) who synthesized the 3-pinanol-2-  
448 hydrogen sulfate.

449

## 450 REFERENCES

451 Atkinson, R.; Aschmann, S.M.; Arey, J.; Shorees, B. Formation of OH radicals in the gas phase  
452 reactions of O<sub>3</sub> with a series of terpenes. *J. Geophys. Res.* **1992**, *97*, 6065-6073.

453

454 Atkinson, R. Gas-phase tropospheric chemistry of volatile organic compounds: 1. Alkanes and  
455 alkenes. *J. Phys. Chem. Ref. Data* **1997**, *26*, 215-290.

456

457 Atkinson, R.; Baulch, D.L.; Cox, R.A.; Crowley, J.N.; Hampson, R.F.; Hynes, R.G.; Jenkin, M.E.;  
458 Rossi, M.J.; Troe, J. Evaluated kinetic and photochemical data for atmospheric chemistry: Volume II -  
459 gas phase reactions of organic species. *Atmos. Chem. Phys.* **2006**, *6*, 3625-4055.

460

461 Baker, J.; Arey, J.; Atkinson, R. Formation and reaction of hydroxycarbonyls from the reaction of OH  
462 radicals with 1,3-butadiene and isoprene. *Environ. Sci. Technol.* **2005**, *39*, 4091-4099.

463

464 Budisulistiorini, S.H.; Li, X.; Bairai, S.T.; Renfro, J.; Liu, Y.; Liu, Y.J.; McKinney, K.A.; Martin,  
465 S.T.; McNeill, V.F.; Pye, H.O.T.; Nenes, A.; Neff, M.E.; Stone, E.A.; Mueller, S.; Knote, C.; Shaw,  
466 S.L.; Zhang, Z.; Gold, A.; and Surratt, J.D. Examining the effects of anthropogenic emissions on  
467 isoprene-derived secondary organic aerosol formation during the 2013 Southern Oxidant and Aerosol  
468 Study (SOAS) at the Look Rock, Tennessee, ground site. *Atmos. Chem. Phys. Discuss.* **2015**, *15*,  
469 7365-7417.

470

471 Chan, A.W.H.; Chan, M.N.; Surratt, J.D.; Chhabra, P.S.; Loza, C.L.; Crounse, J.D.; Yee, L.D.; Flagan,  
472 R.C.; Wennberg, P.O.; Seinfeld, J.H. Role of aldehyde chemistry and NO<sub>x</sub> concentrations in secondary  
473 organic aerosol formation. *Atmos. Chem. Phys.* **2010**, *10*, 7169-7188.

474

475 Chan, C.K.; Ha, Z.; Choi, M.Y. Study of water activities of aerosols of mixtures of sodium and  
476 magnesium salts. *Atmos. Environ.* **2000**, *34*, 4795-4803.

477

478 Chen, Z.M.; Wang, H.L.; Zhu, L.H.; Wang, C.X.; Jie, C.Y.; Hua, W. Aqueous-phase ozonolysis of  
479 methacrolein and methyl vinyl ketone: A potentially important source of atmospheric aqueous  
480 oxidants. *Atmos. Chem. Phys.* **2008**, *8*, 2255-2265.

481

482 Claeys, M.; Graham, B.; Vas, G.; Wang, W.; Vermeylen, R.; Pashynska, V.; Cafmeyer, J.; Guyon, P.;  
483 Andreae, M.O.; Artaxo, P.; Maenhaut, W. Formation of secondary organic aerosols through  
484 photooxidation of isoprene. *Science* **2004a**, *303*, 1173-1176.

485 Claeys, M.; Wang, W.; Ion, A.C.; Kourtchev, I.; Gelencsér, A.; Maenhaut, W. Formation of secondary  
486 organic aerosols from isoprene and its gas-phase oxidation products through reaction with hydrogen  
487 peroxide. *Atmos. Environ.* **2004b**, 38, 4093, 4098.  
488  
489 Czoschke, N.M.; Jang, M.; Kamens, R.M. Effect of acidic seed on biogenic secondary organic aerosol  
490 growth. *Atmos. Environ.* **2003**, 37, 4287-4299.  
491  
492 Edney, E.O.; Kleindienst, T.E.; Jaoui, M.; Lewandowski, M.; Offenberg, J.H.; Wang, W.; Claeys, M.  
493 Formation of 2-methyl tetrols and 2-methylglyceric acid in secondary organic aerosol from laboratory  
494 irradiated isoprene/NO<sub>x</sub>/SO<sub>2</sub>/air mixtures and their detection in ambient PM<sub>2.5</sub> samples collected in the  
495 eastern United States. *Atmos. Environ.* **2005**, 39, 5281-5289.  
496  
497 Fang, W.; Gong, L.; Zhang, Q.; Cao, M.; Li, Y.; Sheng, L. Measurements of secondary organic  
498 aerosol formed from OH-initiated photo-oxidation of isoprene using online photoionization aerosol  
499 mass spectrometry. *Environ. Sci. Technol.* **2012**, 46, 3898-3904.  
500  
501 Gaston, C.J.; Riedel, T.P.; Zhang, Z.; Gold, A.; Surratt, J.D.; Thornton, J.A. Reactive uptake of an  
502 isoprene-derived epoxydiol to submicron aerosol particles. *Environ. Sci. Technol.* **2014**, 48, 11178-  
503 11186.  
504  
505 Gómez-González, Y.; Surratt, J.D.; Cuyckens, F.; Szmigielski, R.; Vermeylen, R.; Jaoui, M.;  
506 Lewandowski, M.; Offenberg, J.H.; Kleindienst, T.E.; Edney, E.O.; Blockhuys, F.; Van Alsenoy, C.;  
507 Maenhaut, W.; Claeys, M. Characterization of organosulfates from the photooxidation of isoprene and  
508 unsaturated fatty acids in ambient aerosol using liquid chromatography/(-) electrospray ionization  
509 mass spectrometry. *J. Mass Spect.* **2008**, 43, 371-382.  
510  
511 Guenther, A.; Karl, T.; Harley, P.; Wiedinmyer, C.; Palmer, P.I.; Geron, C. Estimates of global  
512 terrestrial isoprene emissions using MEGAN (Model of Emissions of Gases and Aerosols from  
513 Nature). *Atmos. Phys. Chem.* **2006**, 6, 3181-3210.  
514  
515 Hallquist, M.; Wenger, J.C.; Baltensperger, U.; Rudich, Y.; Simpson, D.; Claeys, M.; Dommen, J.;  
516 Donahue, N.M.; George, C.; Goldstein, A.H.; Hamilton, J.F.; Herrmann, H.; Hoffmann, T.; Iinuma,  
517 Y.; Jang, M.; Jenkin, M.E.; Jimenez, J.L.; Kiendler-Scharr, A.; Maenhaut, W.; McFiggans, G.; Mentel,  
518 T.F.; Monod, A.; Prévôt, A.S.H.; Seinfeld, J.H.; Surratt, J.D.; Szmigielski, R.; Wildt, J. The formation,  
519 properties and impact of secondary organic aerosol: current and emerging issues. *Atmos. Chem. Phys.*  
520 **2009**, 9, 5155-5236.  
521  
522 Hansen, A.M.K.; Kristensen, K.; Nguyen, Q.T.; Zare, A.; Cozzi, F.; Nøjgaard, J.K.; Skov, H.; Brandt,  
523 J.; Christensen, J.H.; Ström, J.; Tunved, P.; Krejci, R.; Glasius, M. Organosulfates and organic acids in  
524 Arctic aerosols: Speciation, annual variation and concentration levels. *Atmos. Chem. Phys.* **2014**, 14,  
525 7807-7823.  
526  
527 Hasson, A.S.; Ho, A.W.; Kuwata, K.T.; Paulson, S.E. Production of stabilized Criegee intermediates  
528 and peroxides in the gas phase ozonolysis of alkenes 2. Asymmetric and biogenic alkenes. *J. Geophys.*  
529 *Res. Atmos.* **2001**, 106, 34143-34153.  
530  
531 Henze, D.K.; Seinfeld, J.H. Global secondary organic aerosol from isoprene oxidation. *Geophys. Res.*  
532 *Lett.* **2006**, 33, L09812

533 Iinuma, Y.; Böge, O.; Kahnt, A.; Herrmann, H. Laboratory chamber studies on the formation of  
534 organosulfates from reactive uptake of monoterpene oxides. *Phys. Chem. Chem. Phys.* **2009**, 11, 7985-  
535 7997.

536

537 Inomata, S.; Sato, K.; Hirokawa, J.; Sakamoto, Y.; Tanimoto, H.; Okumura, M.; Tohno, S.; Imamura,  
538 T. Analysis of secondary organic aerosols from ozonolysis of isoprene by proton transfer reaction  
539 mass spectrometry. *Atmos. Environ.* **2014**, 97, 397-405.

540

541 Jang, M.; Czoschke, N.M.; Lee, S.; Kamens, R.M. Heterogeneous atmospheric aerosol production by  
542 acid-catalyzed particle-phase reactions. *Science* **2002**, 298, 814-817.

543

544 Kamens, R.M.; Gery, M.W.; Jeffries, H.E.; Jackson, M.; Cole, E.I. Ozone-isoprene reactions: product  
545 formation and aerosol potential. *Int. J. Chem. Kinet.* **1982**, 14, 955-975.

546

547 Kleindienst, T.E.; Lewandowski, M.; Offenberg, J.H.; Jaoui, M.; Edney, E.O. Ozone-isoprene  
548 reaction: Re-examination of the formation of secondary organic aerosol. *Geophys. Res. Lett.* **2007**, 34,  
549 L01805.

550

551 Kroll, J.H.; Ng, N.L.; Murphy, S.M.; Flagan, R.C.; Seinfeld, J.H. Secondary organic aerosol formation  
552 from isoprene photooxidation. *Environ. Sci. Technol.* **2006**, 40, 1869-1877.

553

554 Kroll, J.H.; Seinfeld, J.H. Chemistry of secondary organic aerosol: formation and evolution of low-  
555 volatility organics in the atmosphere. *Atmos. Environ.* **2008**, 42, 3593-3624.

556

557 Liggio, J.; Li, S.-M. Organosulfate formation during the uptake of pinonaldehyde on acidic sulfate  
558 aerosols. *Geophys. Res. Lett.* **2006**, 33, L13808.

559

560 Lin, Y.-H.; Zhang, Z.; Docherty, K.S.; Zhang, H.; Budisulistiorini, S.H.; Rubitschun, C.L.; Shaw,  
561 S.L.; Knipping, E.M.; Edgerton, E.S.; Kleindienst, T.E.; Gold, A.; Surratt, J.D. Isoprene epoxydiols as  
562 precursors to secondary organic aerosol formation: acid-catalyzed reactive uptake studies with  
563 authentic compounds. *Environ. Sci. Technol.* **2012**, 46, 250-258.

564

565 Lin, Y.-H.; Budisulistiorini, S.H.; Chu, K.; Siejack, R.A.; Zhang, H.; Riva, M.; Zhang, Z.; Gold, A.;  
566 Kautzman, K.E.; Surratt, J.D. Light-absorbing oligomer formation in secondary organic aerosol from  
567 reactive uptake of isoprene epoxydiols. *Environ. Sci. Technol.* **2014**, 48, 12012-12021.

568

569 Mellouki, A.; Teton, S.; Le Bras, G. Kinetics of OH radical reactions with a series of ethers. *Int. J.*  
570 *Chem. Kinet.* **1995**, 27, 791-805.

571

572 Neeb, P.; Kolloff, A.; Koch, S.; Moortgat, G.K. Rate constants for the reactions of methylvinyl ketone,  
573 methacrolein, methacrylic acid, and acrylic acid with ozone. *Int. J. Chem. Kinet.* **1998**, 30, 769-776.

574

575 Ng, N.L.; Kwan, A.J.; Surratt, J.D.; Chan, A.W.H.; Chhabra, P.S.; Sorooshian, A.; Pye, H.O.T.;  
576 Crouse, J.D.; Wennberg, P.O.; Flagan, R.C.; Seinfeld, J.H. Secondary organic aerosol (SOA)  
577 formation from reaction of isoprene with nitrate radicals (NO<sub>3</sub>). *Atmos. Chem. Phys.* **2008**, 8, 4117-  
578 4140.

579

580 Nguyen, T.B.; Bateman, A.P.; Bones, D.L.; Nizkorodov, S.A.; Laskin, J.; Laskin, A. High-resolution  
581 mass spectrometry analysis of secondary organic aerosol generated by ozonolysis of isoprene. *Atmos.*  
582 *Environ.* **2010**, 44, 1032-1042.  
583  
584 Nguyen, T.B.; Roach, P.J.; Laskin, J.; Laskin, A.; Nizkorodov, S.A. Effect of humidity on the  
585 composition of isoprene photooxidation secondary organic aerosol. *Atmos. Chem. Phys.* **2011**, 11,  
586 6931-6944.  
587  
588 Olson, C.N.; Galloway, M.M.; Yu, G.; Hedman, C.J.; Lockett, M.R.; Yoon, T.; Stone, E.A.; Smith,  
589 L.M.; Keutsch, F.N. Hydroxycarboxylic acid-derived organosulfates: Synthesis, stability, and  
590 quantification in ambient aerosol. *Environ. Sci. Technol.* **2011**, 45, 6468-6474.  
591  
592 Pandis, S.N.; Paulson, S.E.; Seinfeld, J.H.; Flagan, R.C. Aerosol formation in the photooxidation of  
593 isoprene and  $\beta$ -pinene. *Atmos. Environ. Part A* **1991**, 25, 997-1008.  
594  
595 Paulot, F.; Crounse, J.D.; Kjaergaard, H.G.; Kroll, J.H.; Seinfeld, J.H.; Wennberg, P.O. Isoprene  
596 photooxidation: New insights into the production of acids and organic nitrates. *Atmos. Chem. Phys.*  
597 **2009**, 9, 1479-1501.  
598  
599 Safi Shalamzari, M.; Ryabtsova, O.; Kahnt, A.; Vermeylen, R.; Hérent, M.-F.; Quetin-Leclercq, J.;  
600 Van Der Veken, P.; Maenhaut, W.; Claeys, M. Mass spectrometric characterization of organosulfates  
601 related to secondary organic aerosol from isoprene. *Rapid Commun. Mass Spectrom.* **2013**, 27, 784-  
602 794.  
603  
604 Sato, K.; Inomata, S.; Xing, J.-H.; Imamura, T.; Uchida, R.; Fukuda, S.; Nakagawa, K.; Hirokawa, J.;  
605 Okumura, M.; Tohno, S. Effect of OH radical scavengers on secondary organic aerosol formation  
606 from reactions of isoprene with ozone. *Atmos. Environ.* **2013**, 79, 147-154.  
607  
608 Schindelka, J.; Iinuma, Y.; Hoffmann, D.; Herrmann, H. Sulfate radical-initiated formation of  
609 isoprene-derived organosulfates in atmospheric aerosols. *Faraday Discuss.* **2013**, 165, 237-259.  
610  
611 Surratt, J.D.; Kroll, J.H.; Kleindienst, T.E.; Edney, E.O.; Claeys, M.; Sorooshian, A.; Ng, N.L.;  
612 Offenberg, J.H.; Lewandowski, M.; Jaoui, M.; Flagan, R.C.; Seinfeld, J.H. Evidence for  
613 organosulfates in secondary organic aerosol. *Environ. Sci. Technol.* **2007a**, 41, 517-527.  
614  
615 Surratt, J.D.; Lewandowski, M.; Offenberg, J.H.; Jaoui, M.; Kleindienst, T.E.; Edney, E.O.; Seinfeld,  
616 J.H. Effect of acidity on secondary organic aerosol formation from isoprene. *Environ. Sci. Technol.*  
617 **2007b**, 41, 5363-5369.  
618  
619 Surratt, J.D.; Gómez-González, Y.; Chan, A.W.H.; Vermeylen, R.; Shahgholi, M.; Kleindienst, T.E.;  
620 Edney, E.O.; Offenberg, J.H.; Lewandowski, M.; Jaoui, M.; Maenhaut, W.; Claeys, M.; Flagan, R.C.;  
621 Seinfeld, J.H. Organosulfate formation in biogenic secondary organic aerosol. *J. Phys. Chem. A* **2008**,  
622 112, 8345-8378.  
623  
624 Surratt, J.D.; Chan, A.W.H.; Eddingsaas, N.C.; Chan, M.; Loza, C.L.; Kwan, A.J.; Hersey, S.P.;  
625 Flagan, R.C.; Wennberg, P.O.; Seinfeld, J.H. Reactive intermediates revealed in secondary organic  
626 aerosol formation from isoprene. *Proc. Natl. Acad. Sci.* **2010**, 107, 6640-6645.

627 Wang, W.; Kourtchev, I.; Graham, B.; Cafmeyer, J.; Maenhaut, W.; Claeys, M. Characterization of  
628 oxygenated derivatives of isoprene related to 2-methyltetrols in Amazonian aerosols using  
629 trimethylsilylation and gas chromatography/ion trap mass spectrometry. *Rap. Commun. Mass*  
630 *Spectrom.* **2005**, 19, 1343-1351.

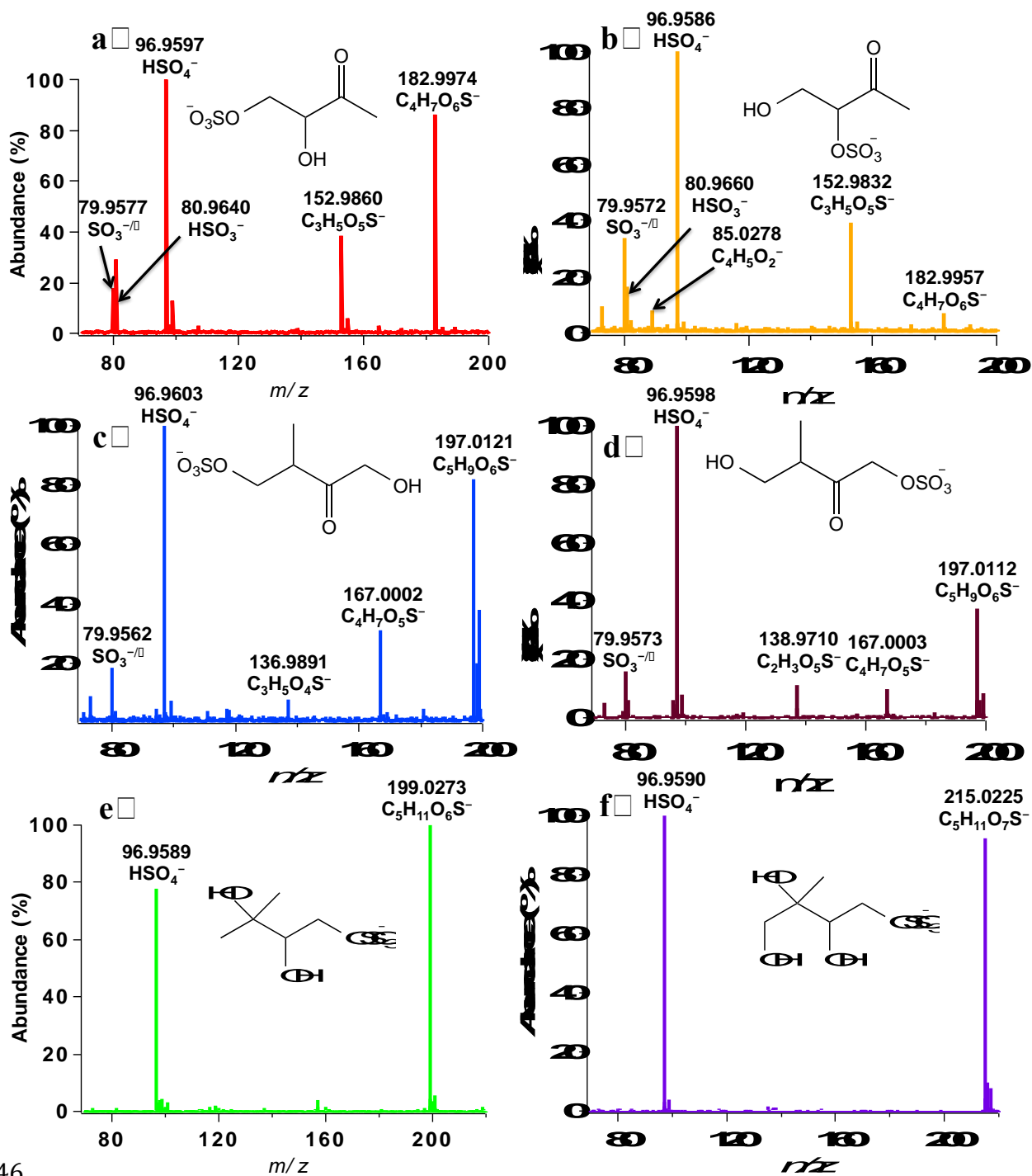
631

632 Xu, L.; Guo, H.; Boyd, C.M.; Klein, M.; Bougiatioti, A.; Cerully, K.M.; Hite, J.R.; Isaacman-  
633 VanWertz, G.; Kreisberg, N.M.; Knote, C.; Olson, K.; Koss, A.; Goldstein, A.H.; Hering, S.V.;  
634 De Gouw, J.; Baumann, K.; Lee, S.-H.; Nenes, A.; Weber, R.J.; Ng, N.L. Effects of anthropogenic  
635 emissions on aerosol formation from isoprene and monoterpenes in the southeastern United States.  
636 *Proc. Natl. Acad. Sci. USA* **2015**, 112, 37-42.

637

638 Zhang, H.; Worton, D.R.; Lewandowski, M.; Ortega, J.; Rubitschun, C.L.; Park, J.-H.; Kristensen, K.;  
639 Campuzano-Jost, P.; Day, D.A.; Jimenez, J.L.; Jaoui, M.; Offenberg, J.H.; Kleindienst, T.E.; Gilman,  
640 J.; Kuster, W.C.; De Gouw, J.; Park, C.; Schade, G.W.; Frossard, A.A.; Russell, L.; Kaser, L.; Jud, W.;  
641 Hansel, A.; Cappellin, L.; Karl, T.; Glasius, M.; Guenther, A.; Goldstein, A.H.; Seinfeld, J.H.; Gold,  
642 A.; Kamens, R.M.; Surratt, J.D. Organosulfates as tracers for secondary organic aerosol (SOA)  
643 formation from 2-methyl-3-buten-2-ol (MBO) in the atmosphere. *Environ. Sci. Technol.* **2012**, 46,  
644 9437-9446.

645

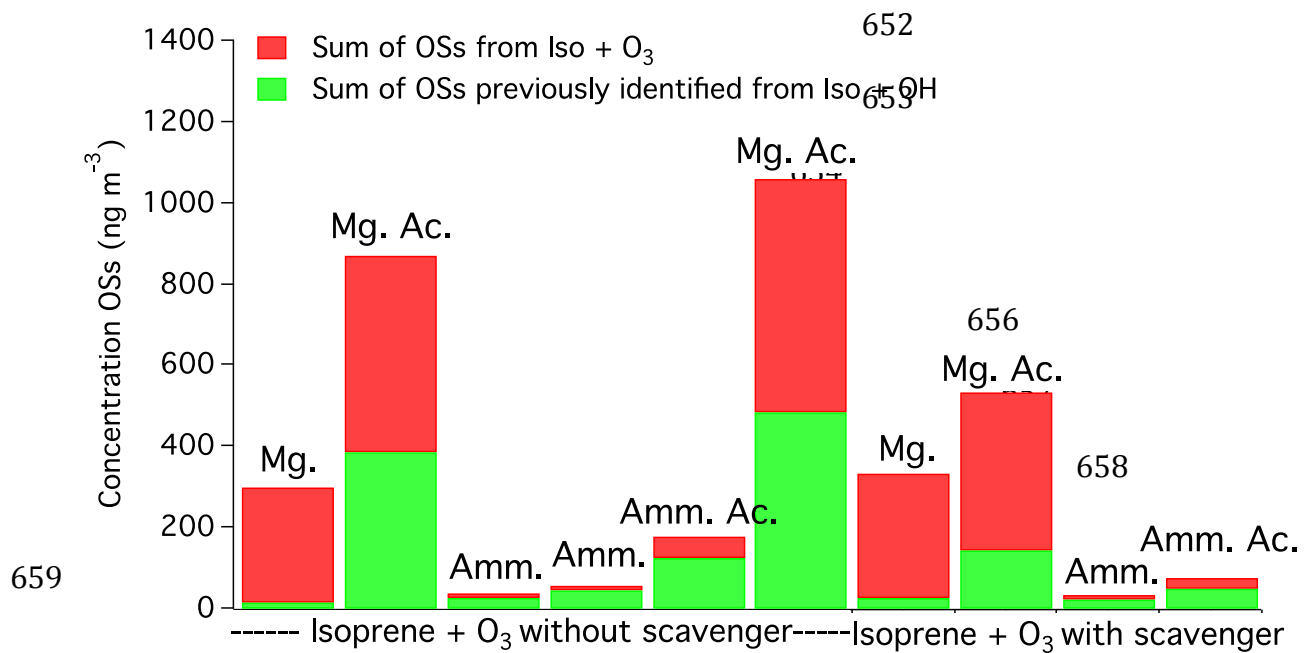


646

647 **Figure 1.** MS<sup>2</sup> spectra obtained for selected isoprene-derived OSs: (a) early- and (b) late-  
 648 eluting  $m/z$  183 ( $C_4H_7O_6S^-$ ), (c) early- and (d) late-eluting  $m/z$  197 ( $C_5H_9O_6S^-$ ), (e)  $m/z$  199  
 649 ( $C_5H_{11}O_6S^-$ ) and (f)  $m/z$  215 ( $C_5H_{11}O_7S^-$ ). Proposed structures for the different parent ions are  
 650 shown as insets on each spectrum.

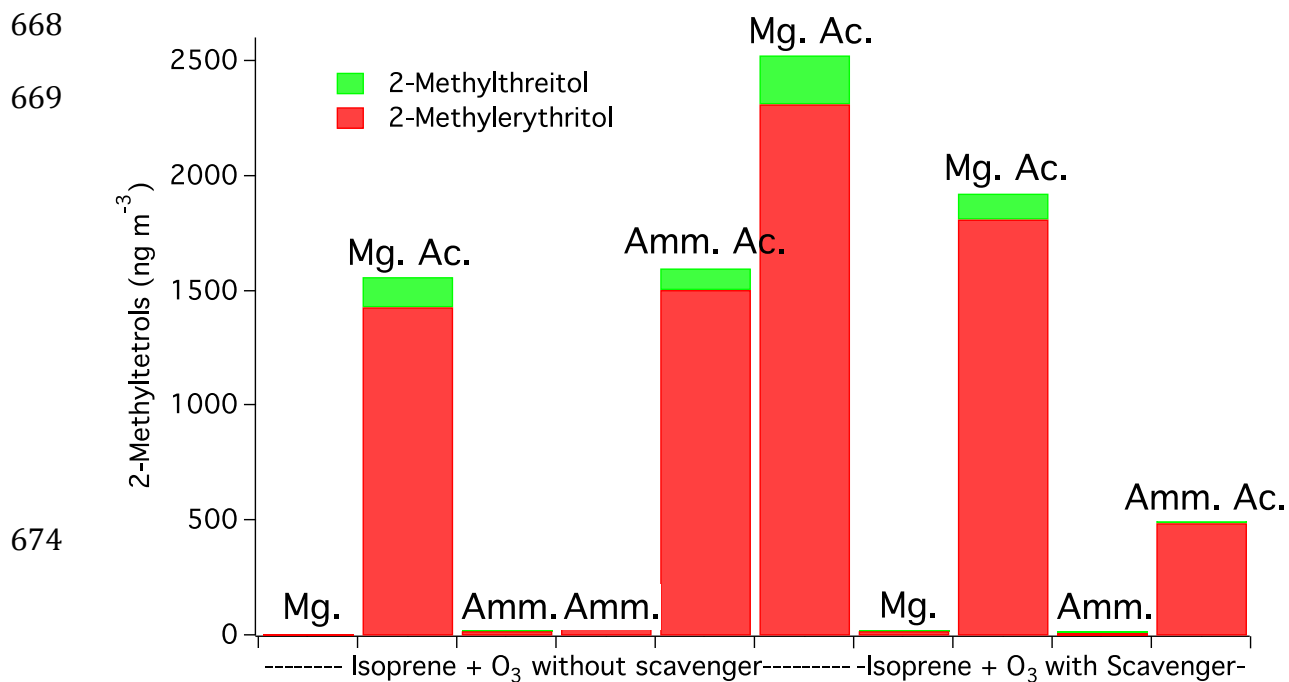
651



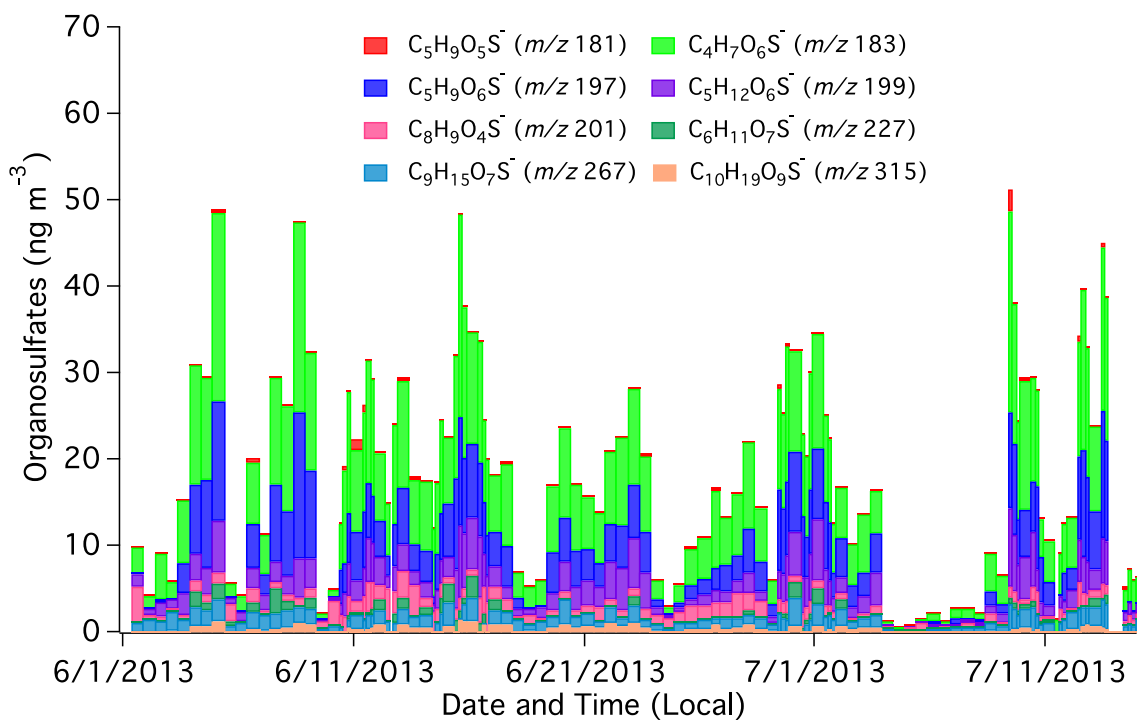


659 **Figure 2.** Quantification of the all identified OSs produced from the chamber isoprene  
 660 ozonolysis (experimental conditions are reported in Tables 1 and 2). Presence of OSs in green  
 661 bars have been previously reported during the photooxidation of isoprene (i.e., OSs reported  
 662 in Table 1), while OSs in red bars corresponds to compounds identified only during the  
 663 isoprene ozonolysis experiments (i.e., OSs in Table 2). *Mg.* and *Amm.* correspond to  
 664 magnesium and ammonium sulfate seed aerosol, respectively. *Ac.* corresponds to acidified  
 665 sulfate seed aerosol.

667



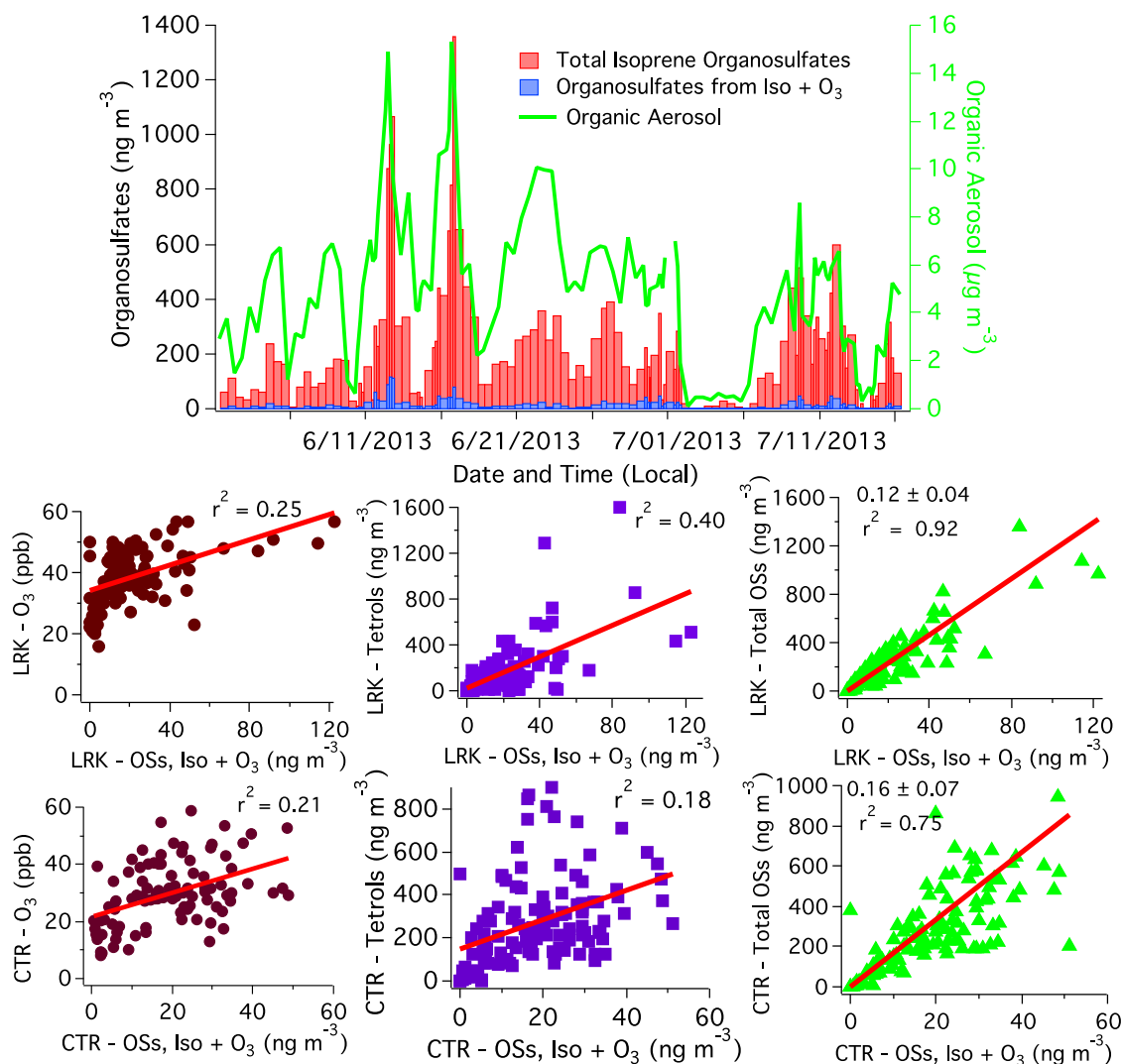
675 **Figure 3.** Quantification of 2-methyltetrols produced from the chamber isoprene ozonolysis  
 676 (experimental conditions are reported in Table 1). *Mg.* and *Amm.* correspond to magnesium  
 677 and ammonium sulfate seed aerosol, respectively. *Ac.* corresponds to acidified sulfate seed  
 678 aerosol.



679

680 **Figure 4.** Temporal variations of OSs from isoprene ozonolysis-only at the CTR site during  
 681 the 2013 SOAS campaign.

682



683

684 **Figure 5.** Temporal variations of OSs identified in the isoprene ozonolysis-only experiment

685 and the sum of all OSs identified from isoprene oxidation (i.e., by OH and O<sub>3</sub>) at the LRK site

686 during the 2013 SOAS campaign (upper plot). Organic aerosol concentrations were measured

687 by an Aerodyne Aerosol Chemical Speciation Monitor (ACSM) (Budisulistiorini et al., 2015).

688 and Bottom plots show correlations of the sum of OSs identified from isoprene ozonolysis-

689 only experiments with ozone (brown markers), 2-methyltetrols (purple markers) and total

690 isoprene OSs (green markers) from both CTR and LRK sites.

691

692 **Table 1.** Summary of experimental conditions and quantification of OSs from isoprene  
 693 ozonolysis that have previously been identified in isoprene photooxidation experiments  
 694 (Surratt et al., 2008).

		Sulfate seed aerosol									
		Mg.	Mg. Ac.	Amm.	Amm.	Amm. Ac.	Mg. Ac.	Mg.	Mg. Ac.	Amm.	Amm. Ac.
Scavenger		-----Yes-----					-----No-----				
[Isoprene] (ppb)		108	105	104	104	97	96	99	102	100	103
[O <sub>3</sub> ] (ppb)		118	123	134	134	117	133	118	130	115	126
[M - H] <sup>-</sup>	(m/z)	Mass concentration (ng m <sup>-3</sup> )									
C <sub>3</sub> H <sub>5</sub> O <sub>5</sub> S <sup>-</sup>	(152.9861) <sup>a</sup>	4.1	30.4	7.5	7.5	9.8	57.5	2.8	32.3	6.7	5.0
C <sub>3</sub> H <sub>5</sub> O <sub>6</sub> S <sup>-</sup>	(168.9820) <sup>a</sup>	<i>N.d.</i>	<i>N.d.</i>	5.9	3.5	14.9	9.1	<i>N.d.</i>	<i>N.d.</i>	4.8	2.1
C <sub>5</sub> H <sub>9</sub> O <sub>7</sub> S <sup>-</sup>	(213.0071) <sup>a</sup>	<i>N.d.</i>	35.1	2.3	7.4	7.1	37.9	<i>N.d.</i>	12.4	<i>N.d.</i>	<i>N.d.</i>
C <sub>5</sub> H <sub>11</sub> O <sub>7</sub> S <sup>-</sup>	(215.0225) <sup>a</sup>	12.8	320.7	12.7	28.8	94.5	390.5	24.1	98.9	10.7	41.0

695 <sup>a</sup> Quantified using synthesized IEPOX-derived OS. Different isomers for one ion have been summed;  
 696 *N.d.*: not detected. Mg. and Amm. correspond to magnesium and ammonium sulfate seed aerosol,  
 697 respectively. Ac. corresponds to acidified sulfate seed aerosol.  
 698

699 **Table 2** Summary of experimental conditions and quantification of OSs from isoprene  
700 ozonolysis not reported as products of isoprene photolysis.

		<b>Sulfate seed aerosol</b>									
		Mg.	Mg. Ac.	Amm.	Amm.	Amm. Ac.	Mg. Ac.	Mg.	Mg. Ac.	Amm.	Amm. Ac.
<b>Scavenger</b>		-----Yes-----					-----No-----				
<b>[Isoprene] (ppb)</b>		108	105	104	104	97	96	99	102	100	103
<b>[O<sub>3</sub>] (ppb)</b>		118	123	134	134	117	133	118	130	115	126
<b>[M - H]<sup>-</sup></b>	<b>(m/z)</b>	<b>Mass concentration (ng m<sup>-3</sup>)</b>									
C <sub>4</sub> H <sub>7</sub> O <sub>6</sub> S <sup>-</sup>	(182.9957) <sup>b,*</sup>	7.1	67.4	3.4	4.6	21.6	101.7	<i>N.d.</i>	53.4	7.4	16.3
C <sub>5</sub> H <sub>11</sub> O <sub>6</sub> S <sup>-</sup>	(199.0273) <sup>a,*</sup>	<i>N.d.</i>	12.4	<i>N.d.</i>	<i>N.d.</i>	1.1	22.1	<i>N.d.</i>	14.5	<i>N.d.</i>	0.4
C <sub>5</sub> H <sub>7</sub> O <sub>5</sub> S <sup>-</sup>	(179.0010) <sup>a</sup>	<i>N.d.</i>	5.7	<i>N.d.</i>	<i>N.d.</i>	1.8	3.7	<i>N.d.</i>	<i>N.d.</i>	<i>N.d.</i>	<i>N.d.</i>
C <sub>5</sub> H <sub>9</sub> O <sub>5</sub> S <sup>-</sup>	(181.0168) <sup>a</sup>	<i>N.d.</i>	4.1	<i>N.d.</i>	<i>N.d.</i>	<i>N.d.</i>	9.1	<i>N.d.</i>	7.8	<i>N.d.</i>	<i>N.d.</i>
C <sub>5</sub> H <sub>9</sub> O <sub>6</sub> S <sup>-</sup>	(197.0121) <sup>b</sup>	<i>N.d.</i>	82.5	2.2	<i>N.d.</i>	12.5	115.9	<i>N.d.</i>	28.5	0.6	4.0
C <sub>8</sub> H <sub>9</sub> O <sub>4</sub> S <sup>-</sup>	(201.0209) <sup>b</sup>	273.8	294.9	7.3	6.3	5.5	276.6	307.9	278.2	4.5	5.5
C <sub>6</sub> H <sub>11</sub> O <sub>7</sub> S <sup>-</sup>	(227.0215) <sup>a</sup>	<i>N.d.</i>	2.5	7.3	<i>N.d.</i>	0.7	4.2	<i>N.d.</i>	0.7	<i>N.d.</i>	<i>N.d.</i>
C <sub>9</sub> H <sub>13</sub> O <sub>6</sub> S <sup>-</sup>	(249.0434) <sup>c</sup>	0.3	1.6	<i>N.d.</i>	<i>N.d.</i>	0.6	2.8	<i>N.d.</i>	1.8	0.3	0.4
C <sub>9</sub> H <sub>15</sub> O <sub>7</sub> S <sup>-</sup>	(267.0531) <sup>c</sup>	<i>N.d.</i>	3.1	<i>N.d.</i>	<i>N.d.</i>	<i>N.d.</i>	6.5	<i>N.d.</i>	0.9	<i>N.d.</i>	<i>N.d.</i>
C <sub>10</sub> H <sub>19</sub> O <sub>9</sub> S <sup>-</sup>	(315.0739) <sup>c</sup>	<i>N.d.</i>	6.7	<i>N.d.</i>	<i>N.d.</i>	3.2	9.1	<i>N.d.</i>	1.4	<i>N.d.</i>	0.6
C <sub>13</sub> H <sub>11</sub> O <sub>10</sub> S <sup>-</sup>	(359.0072) <sup>c</sup>	<i>N.d.</i>	4.0	<i>N.d.</i>	<i>N.d.</i>	<i>N.d.</i>	8.4	<i>N.d.</i>	0.9	<i>N.d.</i>	<i>N.d.</i>
C <sub>15</sub> H <sub>15</sub> O <sub>12</sub> S <sup>-</sup>	(419.0329) <sup>c</sup>	<i>N.d.</i>	0.9	<i>N.d.</i>	<i>N.d.</i>	<i>N.d.</i>	1.9	<i>N.d.</i>	0.4	<i>N.d.</i>	<i>N.d.</i>

701 <sup>a</sup> Quantified using propylsulfate; <sup>b</sup> quantified using authentic IEPOX-OS; <sup>c</sup> quantified using authentic OS  
702 (monoterpenes, OS-249). Different isomers for one ion have been summed; *N.d.*: not detected. Mg. and Amm.  
703 correspond to magnesium and ammonium sulfate seed aerosol, respectively. Ac. corresponds to acidified sulfate  
704 seed aerosol. \* Published (Safi Shalamzari et al., 2013).